

## Temperature-dependent lattice dynamics and equations of state of solid hydrogen\*†

A. B. Anderson†

Colorado State University, Fort Collins, Colorado 80521

and Theoretical and WX Divisions, University of California, Los Alamos Scientific Laboratory, Los Alamos, New Mexico 87545

J. C. Raich and L. B. Kanney

Colorado State University, Fort Collins, Colorado 80521

(Received 28 June 1976)

A numerical computation of the temperature dependence of the pressure volume relations of fcc parahydrogen was carried out within a somewhat modified self-consistent phonon approximation. The effect of the hard core in the intermolecular potential was treated with a short-range correlation function. The hydrogen Hugoniot, specific heat, and average sound velocities were also calculated and comparison with experimental data was made where possible.

### I. INTRODUCTION

In a previous paper,<sup>1</sup> here referred to as I, the ground-state properties of solid molecular *para* hydrogen and *ortho* deuterium were calculated using the self-consistent phonon approximation (SCPA). The hard-core problem in these quantum solids was treated with a short-range correlation function (SRCF) of the type as proposed by Horner.<sup>2</sup> It was found that of the two pair potentials used in I the *ab initio* pair potential proposed by England, Ethers, Raich, and Danilowicz<sup>3</sup> (EERD) was particularly successful in reproducing the pressure-volume results of Anderson and Swenson<sup>4</sup> in the range from 0–30 kbar. The purpose of this paper is to further investigate the validity of the EERD potential and to attempt to use it to calculate properties of solid molecular hydrogen at finite temperatures.

Unfortunately, the SCPA used in I cannot be applied at finite temperatures without modification. With the inclusion of the SRCF, the approximate method of I is a variational treatment in which the ground-state energy is minimized. In order to obtain temperature-dependent effects it is necessary to calculate the Helmholtz free energy,  $F$ . Therefore for  $T > 0$  we have used an approach suggested by Meissner<sup>5</sup> in which many features of the SCPA are retained. Since the EERD potential has proven to be accurate at  $T = 0$ , a comparison of the temperature-dependent properties of solid molecular hydrogen and deuterium with available experimental data will provide a realistic test of the validity of this approach. The SRCF used in conjunction with the Meissner method is the low-temperature form proposed by Horner as modified in I,

$$f(r) = f_0(r) [A_0 + A_1(r - R_0) + A_2(r - R_0)^2]^{1/2}. \quad (1)$$

The constants  $A_0$ ,  $A_1$ , and  $A_2$  are determined as

in I to ensure that the SRCF does not alter the normalization of the two-particle wave function, the average distance between molecules, and the width of the distribution of any pair of molecules about their equilibrium separation,  $R_0$ .

For reasons given below, the form for  $f_0(r)$  was chosen to be the same as in I,

$$f_0(r) = \exp[-0.5(\sigma b/r)^5], \quad (2)$$

where  $\sigma$  is chosen as the Lennard-Jones potential parameter,  $\sigma = 2.958 \text{ \AA}$ . In I,  $b$  was determined as a function of volume at  $T = 0 \text{ K}$  by minimization of the ground-state energy. Here we have used at higher temperatures the values of  $b$  determined in I. As explained in Sec. III, the use of the zero-temperature SRCF can be justified for hydrogen and deuterium because most of the available experimental data are in the temperature range  $T \ll \Theta_D$ , where  $\Theta_D$  is the Debye temperature.

Using the Meissner method, with the SRCF of Eq. (1), and the EERD potential as given in I, we have calculated the specific heats at constant volume,  $C_v$ , as well as several isotherms. Angle-averaged sound velocities were calculated with this method for  $T > 0$  as well as with the approach of I for  $T = 0$ . To further investigate the validity of the EERD potential we have also calculated the shock Hugoniot of  $\text{H}_2$  and compared it with experiment.

### II. CALCULATIONS AND RESULTS

Meissner<sup>5</sup> has given the exact form of the frequency-independent dynamical matrix as

$$\begin{aligned} \bar{\Phi}_{ij}(\vec{k}) = & \left( \frac{1}{N} \right) \sum_{i \neq j} [1 - \exp(-i\vec{k} \cdot \vec{R}_{ij}^0)] \\ & \times \int d^3r \nabla \nabla V(r) \langle \delta(r - r_{ij}) \rangle, \end{aligned} \quad (3)$$

where  $V(r)$  is the two-body intermolecular interaction,  $R_{ij}^0$  is the equilibrium separation between molecules localized around lattice sites  $i$  and  $j$ , and  $r_{ij}$  is their instantaneous separation. The exact pair correlation function  $\langle \delta(r - r_{ij}) \rangle$  can be written as a Fourier transform and expanded in cumulants

$$\begin{aligned} \langle \delta(r - r_{ij}) \rangle = & (2\pi)^{-3} \int d^3k \exp[i\vec{k} \cdot (\vec{r} - \vec{M}_1)] \\ & \times \exp(-\frac{1}{2}\vec{k} \cdot \vec{M}_2 \cdot \vec{k}) \\ & \times \exp\left(\frac{i}{3!}\vec{k}\vec{k}\vec{k}M_3 + \dots\right), \end{aligned}$$

where the lowest cumulants  $\vec{M}_1$  and  $\vec{M}_2$  are  $\vec{R}_{ij}^0$  and  $\langle \vec{u}_{ij}\vec{u}_{ij} \rangle$ , respectively. The cumulant  $\langle \vec{u}_{ij}\vec{u}_{ij} \rangle$  is the displacement-displacement correlation function  $\bar{D}_{ij}$ . Terms containing third- and higher-order cumulants are then regrouped into a function  $\exp[\phi_{ij}(\nabla)]$  where  $\vec{k}$  has been replaced by  $-i\nabla$ :

$$\langle \delta(r - r_{ij}) \rangle = \exp[\phi_{ij}(\nabla)] g_h^{ij}(r),$$

where

$$g_h^{ij}(r) = [(2\pi)^3 \det \bar{D}_{ij}]^{-1/2} \exp(-\frac{1}{2}\vec{u}_{ij} \cdot \bar{D}_{ij}^{-1} \cdot \vec{u}_{ij})$$

and  $\vec{u}_{ij} = \vec{r} - \vec{R}_{ij}^0$ . The function  $\exp[\phi_{ij}(\nabla)]$  is approximated by  $f_{ij}^2(r)$  where  $f_{ij}(r)$  is given by Eq. (2). Neglecting the dispersive terms arising from the odd derivative anharmonicities, the equation for the phonon frequencies  $\omega_{\vec{k}\lambda}$  and the polarization vectors  $\hat{\epsilon}_{\vec{k}\lambda}$  becomes

$$\begin{aligned} \omega_{\vec{k}\lambda}^2 \hat{\epsilon}_{\vec{k}\lambda} = & \frac{1}{NM} \sum_{ij} [1 - \exp(-i\vec{k} \cdot \vec{R}_{ij}^0)] \\ & \times \int d^3u f_{ij}^2(r) g_h^{ij}(u) \nabla \nabla V(r) \cdot \hat{\epsilon}_{\vec{k}\lambda}. \end{aligned} \quad (4)$$

The displacement-displacement correlation function  $\bar{D}_{ij}$  is then calculated in the usual manner<sup>6-8</sup>

$$\begin{aligned} \bar{D}_{ij} = & \frac{\hbar}{NM} \sum_{\vec{k}\lambda} [1 - \exp(i\vec{k} \cdot \vec{R}_{ij}^0)] \\ & \times \omega_{\vec{k}\lambda}^{-1} \coth(0.5\beta\hbar\omega_{\vec{k}\lambda}) \hat{\epsilon}_{\vec{k}\lambda} \hat{\epsilon}_{\vec{k}\lambda}, \end{aligned} \quad (5)$$

where  $\beta = (k_B T)^{-1}$  and  $k_B$  is the Boltzmann constant, while the Helmholtz free energy retains the usual SCPA form<sup>7,9,10</sup>

$$\begin{aligned} F = & \sum_{\vec{k}\lambda} \left[ \beta^{-1} \ln(2 \sinh 0.5\beta\hbar\omega_{\vec{k}\lambda}) \right. \\ & \left. - \frac{\hbar\omega_{\vec{k}\lambda} \coth(0.5\beta\hbar\omega_{\vec{k}\lambda})}{4} \right] + \frac{1}{2} \sum_{ij} \langle V(r_{ij}) \rangle, \end{aligned} \quad (6)$$

where

$$\langle V(r_{ij}) \rangle = \int d^3u f_{ij}^2(r) g_h^{ij}(u) V(r). \quad (7)$$

Initial values of the phonon frequencies and polarization vectors are given by the harmonic approximation<sup>6</sup> with a fictitious potential chosen to give real frequencies. Then displacement-displacement correlation functions are calculated from Eq. (5). New frequencies and polarization vectors are then determined from Eq. (4). This procedure is then iterated until self-consistency is obtained. As in I the face-centered cubic (fcc) structure was assumed. The reader is referred to I for the numerical details of the calculation.

This method is equivalent to including only the instantaneous contributions to the phonon self-energy,  $\phi_\infty$  (in Horner's representation). The limitations of this approximation have been discussed in some detail by Horner.<sup>9</sup> At low temperatures or high pressures (i.e., when the crystal behaves like a classical crystal) the difference between the Meissner force constants and those which include noninstantaneous contributions to the phonon self-energy ( $\phi_0$ ) are small. Here, the Meissner approach is valid. As the temperature increases or the pressure decreases, this difference increases and the results become more questionable. Horner notes that the difference between  $\phi_\infty$  and  $\phi_0$  is of the order of magnitude of the next-order anharmonic correction to the phonon self-energy (a term proportional to odd derivatives of the potential).<sup>11</sup>

The velocity of sound

$$\lim_{k \rightarrow 0} \frac{\partial \omega_{\vec{k}\lambda}}{\partial \vec{k}}$$

was calculated from the eigenvalue [Eq. (4)]. For small  $|\vec{k}|$  the phonon frequencies  $\omega_{\vec{k}\lambda}$  can be approximated as<sup>12</sup>

$$\omega_{\vec{k}\lambda} = C(\hat{k}, \lambda) |\vec{k}|, \quad (8)$$

where  $C(\hat{k}, \lambda)$  is the velocity of sound. Upon expanding Eq. (4) for small  $|\vec{k}|$  and substituting Eq. (8) for the frequencies, one obtains the eigenvalue equation

$$C^2(\hat{k}, \lambda) \hat{\epsilon}_{\vec{k}\lambda} = (2MN)^{-1} \sum_{ij} (\hat{k} \cdot \vec{R}_{ij}^0)^2 \langle \nabla \nabla V(r) \rangle \cdot \hat{\epsilon}_{\vec{k}\lambda},$$

where the average denoted by the angular brackets is defined by Eq. (7). The angle averaged sound velocity is then given as

$$\begin{aligned} C_\lambda = & (4\pi)^{-1} (2MN)^{-1/2} \\ & \times \int d\Omega \left( \sum_{ij} (\hat{k} \cdot \vec{R}_{ij}^0)^2 \hat{\epsilon}_{\vec{k}\lambda} \cdot \langle \nabla \nabla V(r) \rangle \cdot \hat{\epsilon}_{\vec{k}\lambda} \right)^{1/2}. \end{aligned}$$

The integration over the solid angle  $\Omega$  was performed numerically employing an integration

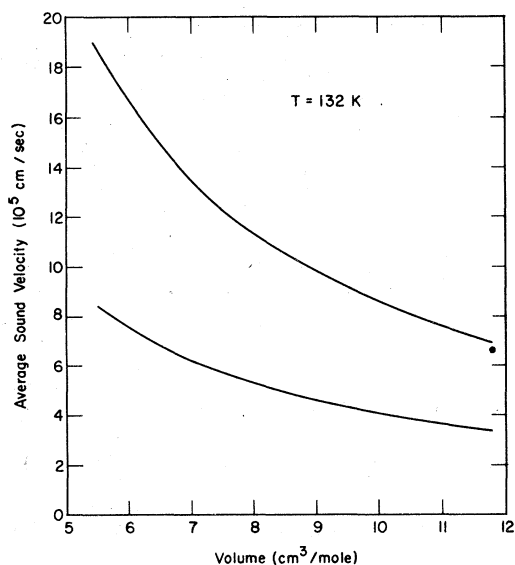


FIG. 1. Angle-averaged sound velocities as a function of molar volume at  $T = 132$  K. Longitudinal and transverse velocities are given by the upper and lower curves, respectively. Experimental longitudinal velocity is from Ref. 20.

scheme proposed by Wallace.<sup>12</sup> Average sound velocities calculated in this way are displayed in Figs. 1–3. The zero-temperature average sound velocities shown in Figs. 4 and 5 were calculated with the zero-temperature theory of I.

The specific heat,  $C_v$ , plotted as a function of temperature in Figs. 6–8, were calculated numerically from the free energies defined by Eq. (6) according to

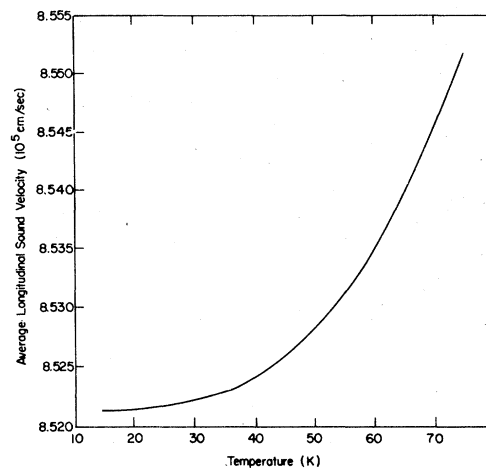


FIG. 3. Angle-averaged longitudinal sound velocities as a function of temperature at a constant volume of  $10$   $\text{cm}^3/\text{mole}$ .

$$C_v = -T \left. \frac{\partial^2 F}{\partial T^2} \right|_v.$$

The functional form used to perform the indicated differentiation was obtained by fitting the calculated free energies to the form

$$F(T) = \sum_{n=1}^L B_n T^{(n-1)}. \quad (9)$$

The  $L$  values of  $B$  were chosen to give the best smooth fit in a least-squares sense to the free energies  $F$ . According to the calorimetry experiments of Ahlers<sup>13</sup> the specific heat of *para* hydro-

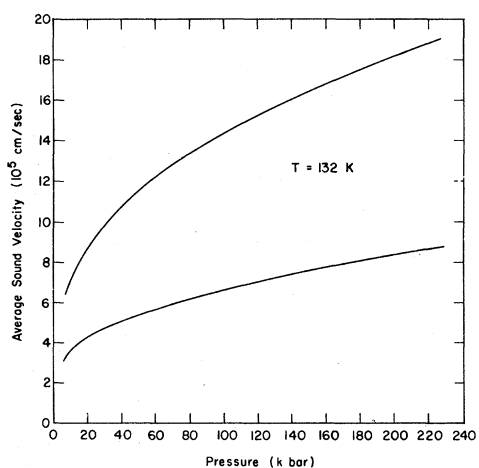


FIG. 2. Angle-averaged sound velocities as a function of pressure at  $T = 132$  K. Longitudinal and transverse velocities are given by the upper and lower curves, respectively.

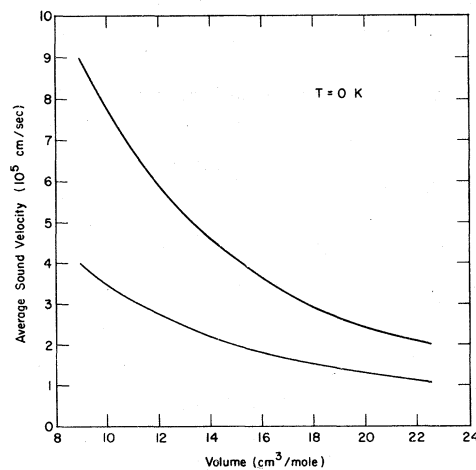


FIG. 4. Angle-averaged sound velocities as a function of molar volume at  $T = 0$ . Longitudinal and transverse velocities are given by the upper and lower curves, respectively.

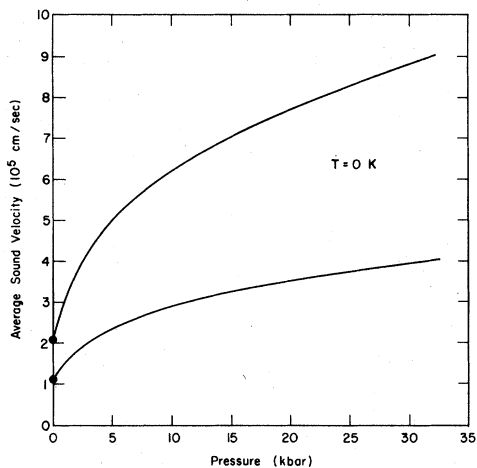


FIG. 5. Angle-averaged sound velocities as a function of pressure at  $T=0$ . Longitudinal and transverse velocities are given by the upper and lower curves, respectively. Experimental points are from Ref. 17.

gen at low pressures has a pure- $T^3$  behavior nearly up to the melting temperature. However, using this approach, we were only able to fit our free energies with relatively poor accuracy to a form which would give a  $T^3$  behavior in  $C_v$  over the range of temperatures shown in Figs. 6–8. In an attempt to improve upon the specific-heat calculations performed above, Eq. (2) was replaced by the high-temperature form proposed by Horner,<sup>2</sup>

$$f_0(r) = \exp[-0.5\beta V(r)]. \quad (10)$$

It was found that for temperatures below 20 K no convergence in the free energy could be reached with this form of  $f_0$ . The form of Eq. (10) is strictly valid for the classical limit and should hold for

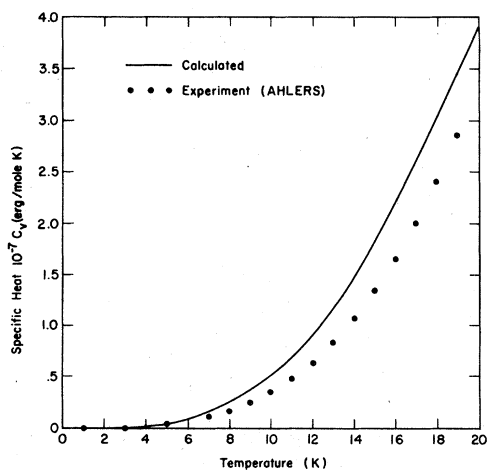


FIG. 6. Specific heat,  $C_v$ , at a molar volume of  $18.73 \text{ cm}^3/\text{mole}$ .

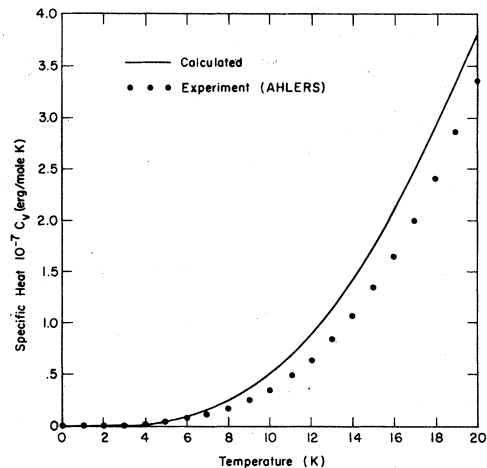


FIG. 7. Specific heat,  $C_v$ , at a molar volume of  $18.63 \text{ cm}^3/\text{mole}$ . Experimental points correspond to a volume of  $18.73 \text{ cm}^3/\text{mole}$ .

temperatures on the order of the Debye temperature. However, at the volumes used in the calculation of our specific-heat curves, the crystal melts well below its Debye temperature.<sup>13</sup>

The isotherm shown in Fig. 9 was calculated from the free energy in a manner similar to the specific-heat calculation. The free energies were fit to the same functional form as Eq. (9), with the temperature replaced by the volume. The pressure is then given as

$$p = - \left. \frac{\partial F}{\partial V} \right|_T.$$

As a further test of the validity of the EERD potential the shock Hugoniot was also calculated. The method employed in the calculation was the

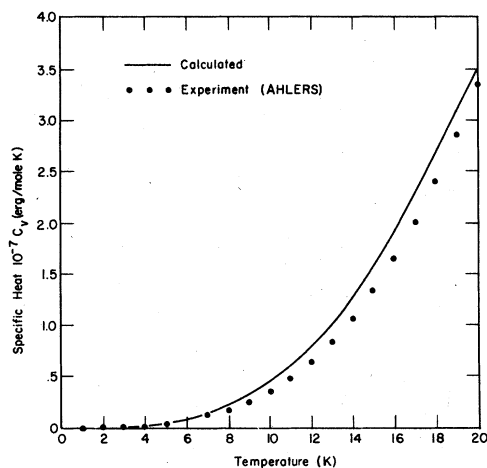


FIG. 8. Specific heat,  $C_v$ , at a molar volume of  $18.26 \text{ cm}^3/\text{mole}$ . Experimental points correspond to a molar volume of  $18.73 \text{ cm}^3/\text{mole}$ .

same as that used by Ross,<sup>14</sup> with the exception that the contributions to the free energy caused by the internal degrees of freedom were calculated with the theory of Pennington and Kobe.<sup>15</sup> For comparative purposes we have also used the potential suggested by Ross. The Hugoniot calculated in this manner appear in Fig. 10 along with the experimental point of van Thiel and Alder.<sup>16</sup>

### III. DISCUSSION AND CONCLUSIONS

As in I where sound velocities were calculated in specific symmetry directions it is seen from Fig. 5 that the EERD potential is successful at  $T=0$  and zero pressure in predicting the angle averaged sound velocities of *para* hydrogen. The experimental points shown in Fig. 5 were measured by Bezuglyi *et al.*<sup>17</sup> in polycrystalline samples of *para* hydrogen and should be considered as angle-averaged sound velocities. More recently Wanner and Meyer<sup>18</sup> have measured sound velocities in a large quantity of normal hydrogen crystals. Their smoothed data for normal hydrogen agreed well with earlier data by Bezuglyi and Minyafaev<sup>19</sup> although the authors of Ref. 18 found somewhat lower values for the longitudinal velocities. The differences between the experimentally measured sound velocities are fairly small (with the exception of Wanner and Meyers's longitudinal velocities) and it is sufficient to use the *para* hydrogen results of Ref. 17 for comparative purposes. It can be seen in Fig. 5 that the agreement is excellent.

The shock Hugoniot shown in Fig. 10 indicates that the EERD potential is probably too "stiff" in the core region. By comparison it is seen that the Ross potential,<sup>14</sup> also investigated in I, pre-

dicts a shock Hugoniot within the error bars of van Thiel and Alder.<sup>16</sup> It is not known to what extent the Trubitsyn-like damping term in the EERD potential might effect the Hugoniot. It is possible that a modification of this term might lower the Hugoniot and still not effect in a serious way the results of I.

Figure 1 indicates that the sound velocities are in fair agreement with the experimental point of Mills *et al.*<sup>20</sup> which was measured in normal hydrogen at 132 °K. Additional sound velocity measurements in solid hydrogen are presently underway and it is hoped that more data will be available in the near future. Curves similar to those of Figs. 1, 2, and 9 were also generated for temperatures of 91 and 200 K. Although the change of temperature yields numerically different values of sound velocities and pressures, the curves appear identical to Figs. 1, 2, and 9 and therefore are not presented here. From Fig. 3 it is observed that the sound velocities, although temperature dependent, change by less than 0.5% over a rather large temperature range at a molar volume of 10 cm<sup>3</sup>. The transverse sound velocities are found to lie on a curve very similar to Fig. 3 with the ordinate rescaled to have a maximum value of 4.132 and minimum value of 4.112.

A comparison of Figs. 3 and 4 shows what must be interpreted as a major failure of the approach used in this paper. The sound velocities of Fig.

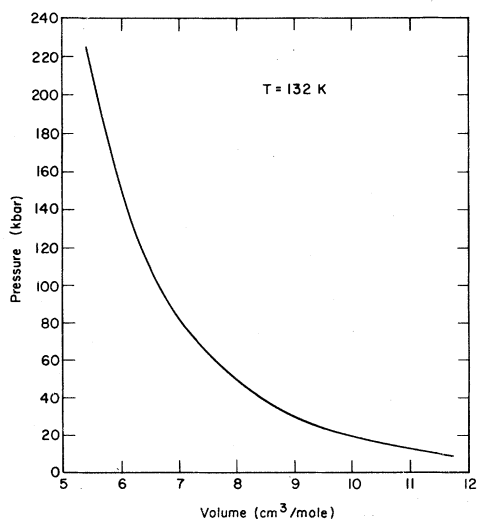


FIG. 9. Isotherm at 132 K.

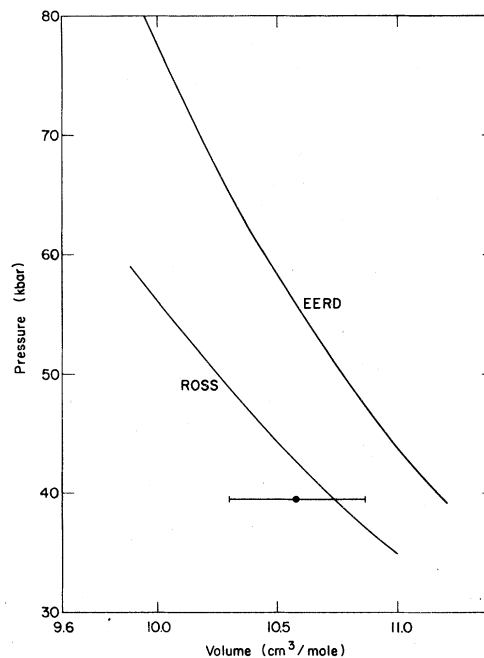


FIG. 10. Shock Hugoniot. Experimental point is from Ref. 16. Initial conditions were  $T = 20.7$  K and  $V = 28.6$  cm<sup>3</sup>/mole.

3 extrapolate into much higher values at zero temperature than are shown in Fig. 4. Also, the present method predicts only a slight temperature dependence of the pressure-volume curves. Although the pressures do increase at fixed volume as a function of temperature, even the pressures at  $T=200$  K are lower than those calculated in I at  $T=0$ . A probable source for these discrepancies is that the free energy of Eq. (6) is too crude an approximation especially when compared to I. This form for the free energy was used with reasonable success by the authors of Ref. 11 to calculate specific heats at high temperature for krypton. They found that this method gave better results than the improved self-consistent phonon approximation<sup>21-23</sup> which has been considered as one of the more successful temperature-dependent theories. Unfortunately their calculation was restricted to a nearest-neighbor model which overemphasizes the effects of the short-range correlations.

Another possible cause for the poor reliability of the isotherms is the particular form chosen for the SRCF. It is reasonable to assume that the low-temperature form given by Eq. (2) is valid at temperatures well below the Debye temperature. This assumption is probably most valid in the calculation of the specific heat where the maximum temperature investigated was 20 K. The Debye temperature as a function of molar volume has been determined by Ahlers.<sup>13</sup> For example, at  $T=0$  K and a volume of  $22.56$  cm<sup>3</sup>/mole,  $\Theta_D$  is 128.1 K. At  $18.73$  cm<sup>3</sup>/mole,  $\Theta_D$  is 189.4 K. At  $T=20$  K and volumes within the range investigated in our specific-heat calculations, the Debye temperature is larger than 100 K. The Debye temperature is known to decrease with increasing temperature at constant volume. At temperatures on the order of 100 K the form for  $f_0$  shown in Eq. (10) is preferred over the one given by Eq. (2).

Figures 6-8 display three specific-heat curves at volumes 18.73, 18.63, and 18.26 cm<sup>3</sup>/mole, respectively. Ahlers's measurements for a volume of 18.73 cm<sup>3</sup>/mole are plotted on all three curves. The calculated values of  $C_v$  in Fig. 6 are approximately 16% too high. Ahlers reports an uncertainty in volume of  $\pm 0.1$  cm<sup>3</sup>/mole. The curve in Fig. 7 corresponds to a decrease in volume of this amount and an increase in accuracy to approximately 13%. With a decrease in volume to 18.26 cm<sup>3</sup>/mole, the curve in Fig. 8 is 4% too high at 20 K. It appears that by decreasing Ahler's reported volume by 2.5% we can calculate specific heats roughly within the 4% total accuracy reported by Ahlers.

In summary, we have continued the investigation of the hydrogen pair potential, proposed by EERD, begun in I, with the calculation of  $T=0$  average sound velocities and the shock Hugoniot. In I it was shown that this potential adequately describes the available low-temperature experimental pressure-volume results, at least to pressures currently attainable by static methods.<sup>4,24</sup> The zero-temperature angle-averaged sound velocities calculated with the method of I are in excellent agreement with the experiment. From the Hugoniot calculation it appears that this potential is not accurate enough at very small intermolecular separations, and should not be used to estimate the insulator-metal transition pressure.

An evaluation of the applicability of the Meissner method for a prediction of temperature-dependent effects in quantum solids is a more difficult problem. A judgment of the validity of the approach is masked by the particular choice for the SRCF. Reasonable success in the calculation of specific-heat curves at low temperatures coupled with the poor pressure-volume results at higher temperatures would indicate that the form for the SRCF may be largely at fault.

The accuracy of the Meissner approach is therefore still a question. At present it appears that a proper choice of SRCF is essential for an adequate description of quantum solids in terms of the Meissner approach.

Another approach to calculate the solid-state properties of hydrogen and deuterium has recently been taken by Goldman.<sup>25</sup> Instead of treating the short-range correlations, as was done in I as well as in this work, Goldman used the self-consistent phonon approximation including cubic anharmonicities to provide an improved treatment of the elastic constants of hydrogen and deuterium. No short-range correlations were included in his calculations. Goldman used a pair potential of the Barker-Pompe<sup>26</sup> form with potential parameters, chosen within the improved self-consistent phonon approximation, to fit the deuterium results of Anderson and Swenson. A comparison of a calculation using the improved self-consistent method with a calculation incorporating hard-core effects in the manner of I employing the same potential would shed additional light on the relative importance of the short-range correlations and cubic anharmonicities for the quantum crystals—hydrogen and deuterium.

The authors are grateful to Dr. Gerald Kerley for supplying the program that calculated the hydrogen Hugoniot.

- \*Work supported by the NSF.
- † Work performed under the auspices of the U. S. ERDA.
- ‡Supported by Associated Western Universities, Inc.
- <sup>1</sup>A. B. Anderson, J. C. Raich, and R. D. Etters, *Phys. Rev. B* **14**, 814 (1976).
- <sup>2</sup>H. Horner, *Z. Phys. (Leipz.)* **242**, 432 (1971).
- <sup>3</sup>W. England, R. Etters, J. Raich, and R. Danilowicz, *Phys. Rev. Lett.* **32**, 758 (1974).
- <sup>4</sup>M. S. Anderson and C. A. Swenson, *Phys. Rev. B* **10**, 5184 (1974).
- <sup>5</sup>G. Meissner, *Phys. Rev. Lett.* **21**, 435 (1968).
- <sup>6</sup>A. A. Maradudin, E. W. Montroll, and G. H. Weiss, *Solid State Physics*, edited by F. Seitz and D. Turnbull (Academic, New York, 1963), Suppl. 3.
- <sup>7</sup>N. S. Gillis, N. R. Werthamer, and T. R. Koehler, *Phys. Rev.* **165**, 951 (1968).
- <sup>8</sup>N. R. Werthamer, *Am. J. Phys.* **37**, 763 (1969).
- <sup>9</sup>H. Horner, in *Dynamical Properties of Solids*, edited by G. K. Horton and A. A. Maradudin (North-Holland, Amsterdam, 1974), Vol. 1, p. 451.
- <sup>10</sup>When the short-range correlations are included according to Horner's formulation, the corresponding corrections are added to the phonon self-energy and are therefore automatically included in the Helmholtz free energy. This free energy retains the same form as when the short-range correlations are absent. As long as  $\phi_\infty$  is approximately equal to  $\phi_0$ , the present expression for the free energy forms a reasonable approximation.
- <sup>11</sup>L. B. Kanney and G. K. Horton, *Phys. Rev. Lett.* **34**, 1565 (1975).
- <sup>12</sup>D. C. Wallace, *Thermodynamics of Crystals* (Wiley, New York, 1972).
- <sup>13</sup>G. Ahlers, thesis (University of California at Berkeley, 1963) (unpublished).
- <sup>14</sup>M. Ross, *J. Chem. Phys.* **60**, 3634 (1974).
- <sup>15</sup>R. E. Pennington and K. A. Kobe, *J. Chem. Phys.* **22**, 1442 (1954).
- <sup>16</sup>M. van Thiel and B. J. Alder, *Mol. Phys.* **10**, 427 (1966).
- <sup>17</sup>P. A. Bezuglyi, R. O. Plakhotin, and L. M. Tarasenko, *Fiz. Tverd. Tela* **13**, 309 (1971) [*Sov. Phys.-Solid State* **13**, 250 (1971)].
- <sup>18</sup>R. Wanner and H. Meyer, *J. Low Temp. Phys.* **11**, 715 (1973).
- <sup>19</sup>P. A. Bezuglyi and R. Kh. Minyafaev, *Fiz. Tverd. Tela* **9**, 624 (1967) [*Sov. Phys.-Solid State* **9**, 480 (1967)].
- <sup>20</sup>R. L. Mills, D. H. Liebenberg, and J. C. Bronson (unpublished).
- <sup>21</sup>M. L. Klein and G. K. Horton, *J. Low Temp. Phys.* **9**, 151 (1972).
- <sup>22</sup>M. L. Klein, V. V. Goldman, and G. K. Horton, *J. Phys. Chem. Solids* **31**, 2441 (1970).
- <sup>23</sup>V. V. Goldman, G. K. Horton, and M. L. Klein, *Phys. Rev. Lett.* **21**, 1527 (1968).
- <sup>24</sup>J. W. Stewart, *J. Phys. Chem. Solids* **1**, 146 (1956).
- <sup>25</sup>V. V. Goldman, *J. Low Temp. Phys.* **24**, 297 (1976).
- <sup>26</sup>J. A. Barker and A. Pompe, *Australian J. Chem.* **21**, 1683 (1968).